Quasibound States and Evidence for a Spin 1 Kondo Effect in Asymmetric Quantum Point Contacts

Hao Zhang,[1] Phillip M. Wu,[2] and Albert M. Chang[1]

[1] *Department of Physics, Duke University, Physics Building,*
Science Drive, Durham, North Carolina 27708, USA
[2] *Division of Solid State Physics and The Nanometer Structure Consortium,*
Lund University, Box 118, S - 22100 Lund, Sweden

(Dated: November 13, 2012)

arXiv:1211.2269v1 [cond-mat.mes-hall] 10 Nov 2012

Linear conductance below $2e^2/h$ shows resonance peaks in highly asymmetric quantum point contacts (QPCs). As the channel length increases, the number of peaks also increases. At the same time, differential conductance exhibits zero bias anomalies (ZBAs) in correspondence with every other peak in the linear conductance. This even odd effect, observable in the longer channels, is consistent with the formation of quasi-localized states within the QPC. In rare cases, triple peaks are observed, indicating the formation of a spin one Kondo effect when the electron filling number is even. Changing the gate voltage tunes this spin triplet to a singlet which exhibits no ZBA. The triple-peak provides the first evidence suggestive of a spin singlet triplet transition in a QPC, and the presence of a ferromagnetic spin interaction between electrons.

The conductance of a quantum point contact(QPC), a quasi one dimensional quantum wire, is quantized in units of $G_0 = 2e^2/h$.[1,2] This can be understood within a single particle picture: the density of states cancels the velocity yielding a unit conductance of G_0 for each subband, with the inclusion of spins. Thus, the total conductance only depends on the number of occupied subbands. However, an additional bump near $0.7G_0$ has drawn much attention as an indication of nontrivial interaction physics[3]. Among the many theoretical proposals[4], a possible explanation for this 0.7 effect is the formation of a quasi-bound state due either to correlation effects,[5–7] or to a momentum mismatch.[8] In a previous paper[9], we presented evidence for quasibound states in QPCs with a highly asymmetric geometry, e.g. observation of sharp resonances and destruction of the lowest G_0 plateau, as well as non-Fermi-liquid temperature evolution of resonance peaks below G_0. Here we report a systematic study on the channel length dependence for several of these unusual features.

We will first demonstrate that the number of conductance resonances increases with an increase in the channel length. This behavior has long been predicted based on quasibound-states formation,[10,11] but yet to be observed experimentally. In a traditional symmetric QPC, the adiabatic potential profile reduces momentum mismatch, minimizing the back-scattering necessary for the formation of the quasibound states[12]. Even with lithographically sharp split gates, the profile can still be smooth due to screening from the long range Coulomb interaction. Our asymmetric QPCs are apparently less adiabatic, leading to an enhancement of the probability for electrons bouncing back and forth from reflections at the entrance and exit of the QPC. Such reflections then give rise to the quasibound states and conductance resonances. In addition to the linear conductance, the differential conductance (dI/dV) was systematically studied. The zero bias anomaly (ZBA) in the dI/dV can be correlated to the linear conductance peaks. In most cases for longer channels $\geq 500nm$, the ZBA is observed for every other linear conductance peak, reminiscent of the even-odd Kondo effect in quantum dots,[13,14] Thus, each successive linear conductance peak corresponds to adding an electron into the quasibound states. However, when the filling number is even, some dI/dV curves exhibit triple peaks near zero bias. This suggests the formation of a spin 1 (triplet) Kondo state instead of a spin 0 (singlet) state. This spin 1 Kondo may arise due to the presence of a ferromagnetic electron spin coupling.[8] By tuning the gate voltage, t was possible to remove the triple-peak and cause a transition to a singlet state. Tuning further

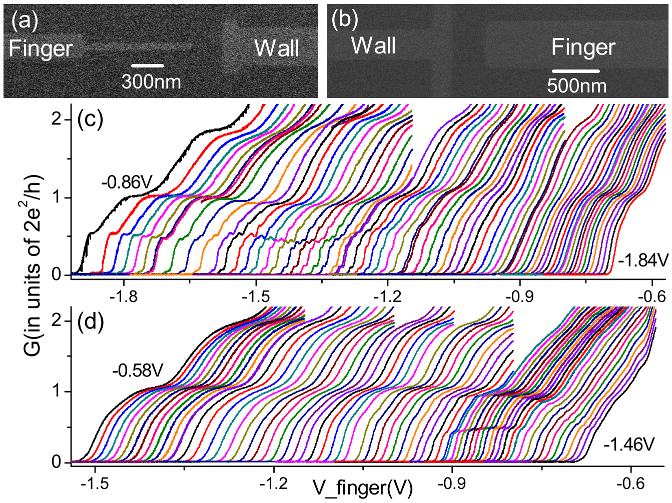

FIG. 1. (Color online)(a),(b) SEM images of two QPCs which have 100nm and 500nm channel lengths, respectively. (c) Conductance of a QPC with a 500nm long channel and 300nm gap. V_{wall} is $-0.86V$ for the leftmost curve(black) and $-1.84V$ for the rightmost (red), and (d) conductance for a QPC with a 1000nm long channel and 300nm gap. $V_{wall} = -0.58V$ for the leftmost(black) and $-1.46V$ for the rightmost(black). The temperature is 4.2 K.

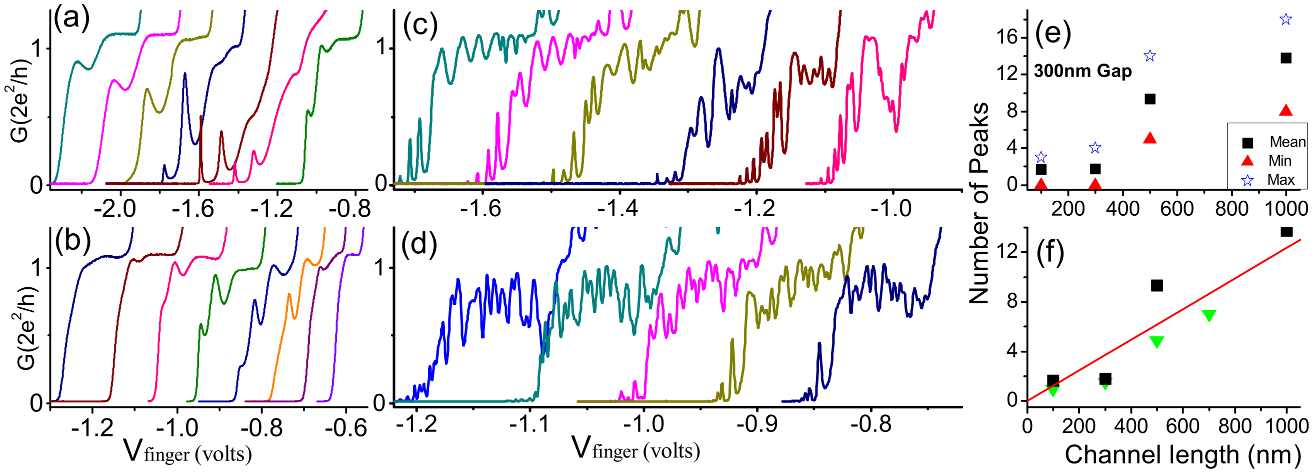

FIG. 2. (Color online)(a)-(d) conductance of 100, 300, 500, and 1000 nm channel length QPCs with 300nm gap. Correspondingly, the leftmost curve has $V_{wall} = -0.91, -0.71, -0.59$ and $-0.59V$ while the rightmost $V_{wall} = -1.47, -1.83, -1.56$ and $-1.23V$. Number of peaks below G_0 vs. channel length: (e) for 300nm gap, and (f) mean number for 250 nm and 300 nm gap.

to an odd filling by adding or removing an electron, a single-peak ZBA emerges instead.

Two set of samples, with split-gate gaps of $300nm$ and $250nm$, were fabricated by electron bem lithography, evaporation of the Cr/Au surface gates, and lift-off. For each set of a fixed gap, channel lengths varying from $100nm$ to $\sim 1000nm$ were defined within a $50\mu m \times 50\mu m$ area of a single chip. In the GaAs/AlGaAs heterostructure crystal, the two dimensional electron gas (2DEG) is located $80nm$ below the surface. The carrier density and mobility are $3.8 \times 10^{11} cm^{-2}$ and $9 \times 10^5 cm^2/Vs$, respectively, giving an electron mean-free-path $\sim 9\mu m$. An excitation voltage $V_{ac} = 10\mu V$ with frequency $17.3Hz$ was applied across the QPC, and the current was measured in a PAR124A lock-in amplifier after conversion to a voltage using an Ithaco 1201 current preamplifier.

Fig.1(a)(b) show typical gate geometries of our QPCs. Unlike conventional QPCs which have two symmetric finger split-gates, we replace one finger with a relatively long wall to introduce asymmetry. The width of the finger gate defines the lithographic channel length, and the gap is the separation between the wall and finger. By applying negative voltages to the wall and finger gates, the 2DEG is depleted underneath, forming the QPC. Each conductance trace was measured by fixing the wall voltage (V_{wall}) while sweeping the finger voltage (V_{finger}). Figs. 1(c) and (d) show conductance traces at 4.2 K for the $500nm$ and $1000nm$ channels with a 300 nm gap. Different traces correspond to different fixed V_{wall}. At this relatively high temperature, the quantized plateaus are already well-defined, indicating that the transport is ballistic. For both devices, as V_{wall} is decreased in steps from the left traces to the right, the $1 \times G_0$ plateau disappears and then reappears at more negative V_{wall} values toward the right. Our previous work[9] reported this suppression of G_0 plateau for 100nm channel length down to 300 mK. Here we find that it is also observable in longer channels. Intriguingly, below G_0, there is a strong bump series near $0.5G_0$ at this high temperature. However, this $0.5G_0$ series was only present in these two QPCs, indicating it is sensitive to the gate parameters and precise channel shape.

At the lower temperature of $\sim 300mK$, the curves develop many oscillations. For clarity, in Figs. 2(a)-(d) we present $\sim 1/8$ of the curves measured for the $300nm$ gap QPC set. The $250nm$ gap QPCs exhibit similar resonances. Note that as the length increases, the number of peaks below the first plateau appears to increase, while at the same time, the typical peak width narrows. Moreover, the spacing between peaks near close to threshold is consistent with the Coulomb charging energy estimates from the channel capacitance to the surroundings. Overall, thermal cycling laterally shifts the curves and changes the details, but the main behavior remains consistent. At $300mK$, the suppression of the $1 \times G_0$ first plateau is clearly seen in (a)(c), but weaker in (b). For each channel length we tabulate the number of peaks below G_0 for each of the ~ 50 curves, and present the statistics in Fig. 2(e)(f). In (e) each (black) square point represents the mean number of peaks for a given channel length in the $300nm$ gap set. (Blue) triangles and (red) circles represent the maximum and minimum number, respectively. In (f), the mean numbers for both $300nm$ and $250nm$ gap are plotted.

The resonances versus channel length, reflected both in the raw traces and the statistics in Fig. 2, clearly demonstrate that the number of resonances increases with, and is approximately proportional to the length. This behavior contrasts with symmetric QPCs as long as $2\mu m$ in length, which show no resonance at all.[15] The conductance peaks can be motivated within a single-particle picture, neglecting interaction, as resulting from quasibound states. When scanning V_{finger}, the relative Fermi level within the first subband, defined as the dis-

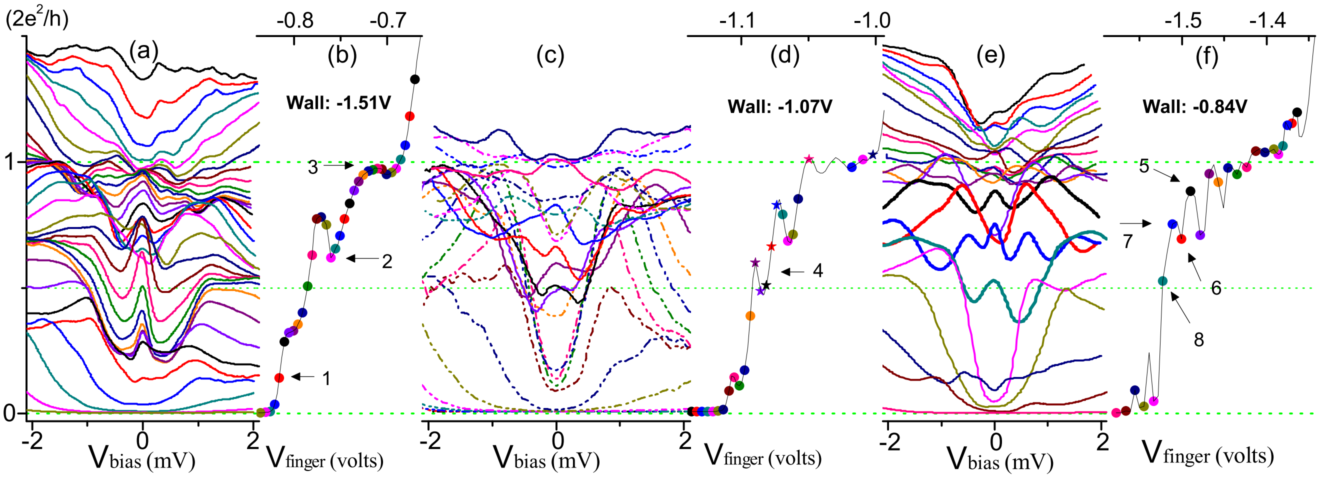

FIG. 3. (Color online)(a) dI/dV for 300nm channel,300nm gap with fixed $V_{wall} = -1.51V$ while sweeping V_{bias}(X axis) and V_{finger}(different color).(b) is a plot the center(linear conductance) of (a) as a function of V_{finger}. (c),(d) dI/dV 500nm channel, 250nm gap. Star points have ZBA and circular points have no ZBA (e),(f) dI/dV for 500nm channel, 300nm gap. G_0 and $\frac{1}{2}G_0$ are labeled as horizontal doted lines for all plots. See text for details regarding the arrows. The temperature is $300mK$.

tance from the first subband level to the chemical potential, changes, along with the Fermi wavelength. In the simplest scenario, when the Fermi wavelength satisfies $N \cdot \frac{\lambda}{2} = L$, where N is a positive integer and L is the channel length, a tunneling resonance(quasibound state) will form. Longer channels have quasibound states more dense in energy, so more conductance resonances are observed. This simple single particle picture, proposed two decades ago, is based on momentum mismatch (or matching) at the channel entrance and exit.

Recently Song and Ahn included electron interactions and further argued that even with quite smooth potential profile, there can still be a momentum mishmatch and the formation of quasibound states.[8] Intriguingly, similar reproducible resonance features was observed by Senz *et al.* in almost the same gate geometry as ours[16], in a QPC defined by surface oxidation. They did not perform a systematic study, however, and was thus unable to separate out the effects of geometry induced non-adiabatic from those of donor impurities.

The number of resonances and peaks, in principle, should correspond to the number of electrons within the channel. This is only roughly obeyed in our QPCs, despite the approximate proportionality of the number of resonances to the channel length. The precise reason for this lack of exact correspondence is not known at the moment, although a similar situation is also encounter in Ref.[13]. One likely cause is that the observability of resonances depends on having a strong reflection at both ends of the channel. The difficulty in observing resonances in the symmetric geometry seems to indicate the self-consistent potential can be significantly smoothed by the screening effect of the long-range Coulomb interaction. The same trend may be expect even in the asymmetric case. Therefore, it is quite possible that even with the asymmetric geometry, many electrons are added, but fail to produce a corresponding resonance, particularly close to the quantized plateau.

Aside asymmetry, unevenly distributed donors can generate a random potential profile, causing backscattering and conductance peaks, as well as the degradation of the quantization on the plateaus.[17] In our case, degradation of plateau quantization is not observed. All the QPCs show well-defined quantized plateaus at 4.2K. Even at 300mK, the plateaus are very clearly present, albeit with resonance oscillations superimposed. In addition to randomness, imperfect lithography may leave small bumps on the gates which also can cause electron backstactering. For short channels (100 or $300nm$), this is highly unlikely, since they are too short for bumps be present; bumps have typical dimensions of 20-50 nm length-wise, and every $\sim 300nm$ (based on SEM imaging). For the longer channels, the presence of randomly located small bumps will lead to quantum dots of varying sizes, giving conductance peaks of random characteristics and spacings. In our data, the peak positions tend to be quite periodic for all the longer channels. Therefore, gate imperfection should not have a dominant effect. In the end, the source of the reflections is not important. As long as electrons are able to bounce back and forth between two well-defined positions, regularly spaced quasibound states should form. The evenly spaced peaks in V_{finger} means that the energy of quasibound states are evenly spaced, since ΔV_{finger} is roughly proportional to ΔE_f. An even spacing in ΔE_f also indicates that electron interaction cannot be neglected; within the single electron picture, peaks occur periodic in momentum, not in energy.

In Fig. 3, we present the nonlinear conductance (dI/dV) as a function of source-drain bias V_{bias}. For each QPC, only half of the curves are presented for clarity. Panel (a) shows the typical behavior in a short channel QPCs ($100nm$, $300nm$). V_{wall} is held fixed and V_{finger} is increased in steps (bottom to top trace). Each curves is for a different V_{finger}, shown with different colors online. V_{bias} ranges from $-2.1mV$ to $2.1mV$. In panel (b), the center cut of (a), equivalent to the zero-bias linear conductance, is represented a symbol of the same color, are plotted versus V_{finger} on the horizontal axis. The black line which connects all symbols, including those not shown, gives the zero-bias linear conductance at the fixed V_{wall} versus V_{finger}. This linear conductance curve is consistent with the corresponding curve in Fig.2 measured separately. Consistency between upward and downward scanning of V_{bias} enable to rule out spurious signals.

Zero bias peaks (ZBPs) in QPCs, associated with the zero bias anomaly (ZBA), is a nonlinear conductance peak near zero bias discovered by Cronenwett et al.[18]. In their work, the temperature evolution of ZBA could be fitted to the universal Kondo formula which in a manner analogous to the Kondo effect in semiconductor quantum dots.[13,14] Their occurrence thus also points to the quasi-localized state formation within the QPC channel, since the Anderson model permits the presence of a localized magnetic impurity, leading to the Kondo effect. As for our data in Fig.3(a), we can see the ZBA begins at the (red) curve (arrow 1 in (b)), and continues all the way up to the first plateau(arrow 3 in (b)). The amplitude of ZBA has a minimum at the second valley in (b) (arrow 2). Three other short channel QPCs show similar features: ZBAs across a wide range.

In a quantum dot, ZBP is observed when the number of electrons inside the dot is odd, for which the total spin or magnetic moment is nonzero. In most cases, there will be no ZBPs for even filling number.[13] This so called even odd effect is nearly obeyed in our long asymmetric QPCs. Figs. 3(c) and (d) present typical data for a long channel QPC. In (c), the dotted lines are curves without ZBA while the solid lines are curves with ZBA. This ZBA and non-ZBA alternation is also differentiated in (d) using different symbols (star or circular).

A QPC is normally thought of as an open system, which implies electron filling number of the channel should not be a precise, good quantum number. The even-odd effect occurs in a confined system, e.g. quantum dots. The formation of quasi bound-states, indicated by the sharp resonances near threshold and at intermediate conductance ($\sim 0.5G_0$), renders the electron filling number to be a quasi-good quantum number. This makes an even-odd effect possible. As in a quantum dot, our ZBA does not strictly follow the even-odd law. Sometimes it can be appeared to be even-odd-odd or even-even-odd. Near threshold, such behavior can result from the small electron tunneling rate to the leads (Γ). A small Γ suppresses the Kondo temperature exponentially, rendering the ZBA unobservable. On the other end, near the $1 \times G_0$ plateau, the channel is quite opened (almost an open system), and it becomes meaningless to define filling number. This near even-odd effect is, observable in the longer channels ($500nm$, $700nm$ and $1000nm$). In contrast, for the short channels which exhibit only one or two peaks in the linear conductance below G_0, ZBAs are almost everywhere (Fig. 3(a)) beyond the threshold region. This behavior is similar to what that reported in other works in somewhat longer channels.[18–20] This behavior is difficult to understand, unless spin states with $S > 1/2$ can occur.[8]

One feature in Fig. 3(e) is particularly interesting. A (blue) dI/dV curve in of intermediate conductance shows triple peaks near zero bias. Following the linear conductance in (f) and cross referencing with (e), The (black colored) curve or dot, labeled by arrow 5, shows a single ZBP which suggests an odd filling number and a spin 1/2 state. Going past the peak in the linear conductance, the curve (red, arrow 6) shows no ZBA but with two big bumps on the sides, which suggests one electron has popped out and now the filling number is even. The next curve (blue, arrow 7) has triple peaks which is unusual as the filling number is still even. Going further, the curve (green, arrow 8) which sits on a small linear conductance bump, has a ZBA suggests the filling number is now odd again. The (black and green) curves (arrows 5 and 8) have odd filling number with ordinary ZBAs. In between where the filling is even, curves with a triple-peak ZBA transition into those with no-ZBA but with a double-side-peak. We ascribe this to a spin triplet-to-singlet transition. Changing V_{finger} tunes the level spacing ΔE_{level} and also ferromagnetic the electron exchange energy($E_{exchange}$. For the curve at arrow 6 (red), $\Delta E_{level} > E_{exchange}$; the groundstate is a spin singlet and the two electrons will occupy the same orbital level. In this situation, there should be no ZBP, and the two-side bumps correspond to an excitation into the triplet when $e|V_{dc}| = \Delta E_{level} - E_{exchange}$. For the curve at arrow 7 (blue), ferromagnetic coupling dominates: $\Delta E_{level} < E_{exchange}$. The ground-state is a spin triplet, and the two electrons will occupy two different orbital levels with total spin equals to 1. Here, the triple-peak in dI/dV will have a center ZBP due to a partial Kondo screening of the $S = 1$ spin, while the two side peaks correspond to a triplet-to-singlet excitation occurring via a second-order process. Singlet-triplet transition has been observed in semiconductor quantum dots[21], and in C_{60} molecular quantum dots[22], but not as yet in QPCs. Recently, Song and Ahn[8] argued that momentum mismatch can give rise to quasibound states, when Coulomb interaction is taken into account. Furthermore, electrons can have ferromagnetic exchange coupling and obeys Hund's rule while filling the quasibound states. Originally intended to explain the 0.7 effect, it now appears that their calculations also provide a qualitative underpinning to our results.

Our observation of a linear scaling of the number of resonances/oscillations with the channel length in asymmetric QPCs, in conjunction with the ubiquitous occurrence of ZBAs in the dI/dV, provide evidence for the existence of quasi-bound states. These quasi-bound states form as a result of reflections from two well-defined positions, mostly likely at the channel entrance and exit. Long channels tend to show an even-odd effect in the ZBA. In rare cases, a transition between singlet and triplet Kondo behavior, consistent with the singlet-triplet quantum phase transition, can be achieved.

We thank M. Pepper, S. Florens, D. Liu, A. C. Mehta, and H. U. Baranger for useful discussions. Work supported by NSF DMR-0701948.

---

[1] B.J. van Wees, H. van Houten, C. W. J. Beenakker, J. G. Williamson, L. P. Kouwenhoven, D. van der Marel, and C.T. Foxon, Phys. Rev. Lett. **60**, 848 (1988).

[2] D. A. Wharam, T. J. Thornton, R. Newbury, M. Pepper, H. Ahmed, J. E. F. Frost, D. G. Hasko, D. C. Peacock, D. A. Richie, and G. A. C. Jones, J. Phys. C **21**, L209 (1988).

[3] K. J. Thomas, J. T. Nicholls, M. Y. Simmons, M. Pepper, D. R. Mace, and D. A. Ritchie, Phys. Rev. Lett. **77**, 135 (1996).

[4] A. P. Micolich, Journal of Physics: Condensed Matter **23**, 443201 (2011).

[5] Y. Meir, K. Hirose, and N. S. Wingreen", Phys. Rev. Lett. **89**, 196802 (2002).

[6] T. Rejec and Y. Meir, Nature **442**, 900 (2006).

[7] A.D. Güçlü, C.J. Umrigar, Hong Jiang, and Harold U. Baranger, Phys. Rev. B **80**, 201302 (R) (2009).

[8] Taegeun Song and Kang-Hun Ahn, Phys. Rev. Lett. **106**, 057203 (2011).

[9] P. M. Wu, Peng Li, Hao Zhang, and A. M. Chang, Phys. Rev. B **85**, 085305 (2012).

[10] G. Kirczenow, Phys. Rev. B **39**, 10452 (1989).

[11] D. van der Marel and E. G. Haanappel, Phys. Rev. B **39**, 7811 (1989).

[12] Aaron Szafer and A. D. Stone, Phys. Rev. Lett. **62**, 300 (1989).

[13] D. Goldhaber-Gordon, H. Shtrikman, D. Mahalu, D. Abusch-Magder, U. Meirav, and M. A. Kastner, Nature **391**, 156 (1998).

[14] H. Jeong, A. M. Chang, and M. R. Melloch, Science **293**, 2221 (2001).

[15] K. M. Liu, V. Umansky, and S. Y. Hsu, Phys. Rev. B **81**, 235316 (2010).

[16] V. Senz, T. Heinzel, T. Ihn, S. Lindemann, K. Ensslin, W. Wegscheidez, and M. Bichler, Journal of Physics: Condensed Matter **13**, 3831 (2001).

[17] John A. Nixon, John H. Davies, and H.U. Baranger, Phys. Rev. B **43**, 12638 (1991).

[18] S. M. Cronenwett, H. J. Lynch, D. Goldhaber-Gordon, L. P. Kouwenhoven, C. M. Marcus, K. Hirose, N. S. Wingreen, and V. Umansky, Phys. Rev. Lett. **88**, 226805 (2002).

[19] F. Sfigakis, C. J. B. Ford, M. Pepper, M. Kataoka, D. A. Ritchie, and M. Y. Simmons, Phys. Rev. Lett. **100**, 026807 (2008).

[20] Y. Ren, W. W. Yu, S. M. Frolov, J. A. Folk, and W. Wegscheider, Phys. Rev. B **82**, 045313 (2010).

[21] A. Kogan, G. Granger, M. A. Kastner, D. Goldhaber-Gordon, and H. Shtrikman, Phy. Rev. B **67**, 113309 (2003).

[22] "Nicolas Roch, Serge Florens, Vincent Bouchiat, Wolfgang Wernsdorfer, and Franck Balestro, Nature **453**, 06930 (2008).